

Defect Pool Numerical Model in Amorphous Semiconductor Device Modeling Program

M. Rahmouni*, S. Belarbi†

Université des Sciences de la Technologie Mohamed-Boudiaf, El Mnouar, BP 1505, Oran, Algeria

(Received 29 December 2018; revised manuscript received 05 April 2019; published online 15 April 2019)

Amorphous Semiconductor Device Modeling Program (ASDMP), developed by Professor P. Chatterjee and widely validated by experimental results, is a detailed program where the Poisson's equation and the electron and hole continuity equations are simultaneously solved without any simplifying assumption. It takes into account the trapping and recombination kinetic through the gap states. In this program, the density of states is modeled using the standard model (SM). Such a model describes the defects by two Gaussians near the center of the gap and two tails exponentially distributed in energy, and assumes the density of states homogenous in space. The defect pool model (DPM) is an improved model for defect formation in hydrogenated amorphous silicon based on the idea that the a-Si:H network has a large spectrum of local environments at which a defect could be formed. So, these defects choose the sites where their formation energy is minimal and this becomes possible with hydrogen motion.

Using the defect pool approach, we have developed a numerical DPM and inserted it in ASDMP at thermodynamic equilibrium. We have used ASDMP to get the density of states in each position of a solar cell based on a standard *p-i-n* structure. We have shown the effect of doping on defect concentration and studied the impact of the position of Fermi level on the distribution of the density of states. We recognized using ASDMP the key result that negatively charged defects in *n*-type material are situated lower in energy than positively charged defects in *p*-type material even when the correlation energy is positive. We calculated the electric field and the band diagrams at thermodynamic equilibrium both with the DPM and the SM. We showed that the electric field obtained from the DPM is stronger near the interfaces and lower in the bulk where the band diagrams are flatter. This behavior of the electric field calculated with this model is accentuated with the increase of the slope of the valence band tails.

Keywords: Hydrogenated amorphous silicon, Defect pool model, *p-i-n*.

DOI: [10.21272/jnep.11\(2\).02008](https://doi.org/10.21272/jnep.11(2).02008)

PACS numbers: 80.81.Xx, 90.96.Xx

1. INTRODUCTION

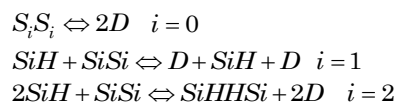
It is well known that a faithful modeling of the distribution of the density of defect states in hydrogenated amorphous silicon is important for a device modeling program to produce correct results. The electronic density of gap states has two components: two tail states which are exponentially distributed in energy and deep states associated with Si dangling bonds (DB). In the standard model (SM), the DB are modeled by two Gaussian functions near the middle of the gap separated by the correlation energy (U). This profile of the density of defect states is assumed to be constant in each layer of a device. Such model leads to positively charged defects in *p*-type material situated at lower energy than negatively charged defects in *n*-type material. However, this is not consistent with experimental results. This has been the model used in the one-dimensional Amorphous Semiconductor Device Modeling Program (ASDMP) [1-2]. The DPM is an improved model developed to calculate the density of DB. It considers that the formation of these DB requires the breaking of weak SiSi bonds [3-6] generally with hydrogen motion. Since, it has been used by many searchers, for example, to analyze the photodegradation effect in a-Si:H [7], photoconductivity [8] and lifetime in heterojunction solar cells [9].

The DPM shows that the calculated density of states depends on specific microscopic reaction involving hydrogen and that the best agreement with exper-

imental result is found for a model where two SiH bonds are involved in each reaction [10-11]. Using this concept we have elaborated a numerical DPM which has been successfully inserted in ASDMP at thermodynamic equilibrium. We present the density of states calculated with ASDMP in each position of a standard *p-i-n* solar cell. We therefore investigate the impact of the density of state profile on the outside parameters in thermodynamic equilibrium.

2. THE DEFECT POOL MODEL

According to the DPM, the density of dangling bonds is based on chemical equilibrium between the weak bonds and the formed dangling bonds. The microscopic reactions describing these processes are [10]:



SiSi are the weak bonds and i is the number of SiH bonds involved in each reaction.

The calculation of the defect density $D(E)$ at energy E requires the defect chemical potential (the free-energy change per defect). It is given by the expression $\mu_d = \langle e \rangle - kT_s_e - kT_s_H$, where $\langle e \rangle$ is the mean energy of the electrons in the dangling bond state depending on the probability of this defect being in each of its three

* Mawahib.rahmouni@univ-usto.dz

† Mansouri_souad2002@yahoo.fr

charge states, s_e is the entropy associated with the electron occupation of the defect and s_H is the entropy due to the hydrogen involvement when $i \neq 0$. This leads to the following expression of the chemical potential:

$$\mu_d(E) = E + kT \ln\left(\frac{f^0(E)}{2}\right) + \frac{ikT}{2} \ln\left(\frac{iD(E)}{2HP(E)}\right), \quad (1)$$

where $f^0(E)$ is the probability of the dangling bond being occupied by zero electrons. H is the concentration of hydrogen and $P(E)$ is the energy distribution of the dangling bonds (the defect pool function). This is caused by the disorder of the amorphous silicon and it is assumed to be Gaussian

$$P(E) = \frac{1}{\sigma\sqrt{2\pi}} \exp\left(-\frac{(E - E_p)^2}{2\sigma^2}\right). \quad (2)$$

Here, σ is the pool width and E_p is the most probable energy in the distribution of available sites for defect formation.

Identifying the weak-bond states with the valence band-tail, the calculation leads to the following expression of the density of states at equilibrium:

$$D(E) = \gamma \left(\frac{2}{f^0(E)}\right)^{\frac{\rho kT}{E_{v0}}} P\left(E + \frac{\rho\sigma^2}{E_{v0}}\right), \quad (3)$$

where

$$\gamma = \left(\frac{N_{v0} 2E_{v0}^2}{2E_{v0} - kT}\right)^\rho \left(\frac{i}{2H}\right)^{\rho-1} \exp\left(\frac{-\rho}{E_{v0}}(E_p - E_v - \frac{\rho\sigma^2}{2E_{v0}})\right), \quad (4)$$

$$\rho = \frac{2E_{v0}}{2E_{v0} + ikT}, \quad (5)$$

N_{v0} is the density of tail states extrapolated to the valence band and E_{v0} is the characteristic energy of the exponential.

This density of states is assumed to be frozen-in at temperatures above the equilibration temperature T^* .

$D(E)$ is divided into three components of different charge density:

$$\begin{aligned} D^+(E) &= D(E)f^+(E), \\ D^0(E) &= D(E)f^-(E), \\ D^-(E) &= D(E)f^-(E), \end{aligned} \quad (6)$$

where f^+ and f^- are the occupation functions of amphoteric DB occupied by zero, one or two electrons, respectively.

3. SIMULATION PROGRAM

The detailed one-dimensional Amorphous Semiconductor Device Modeling Program (ASDMP) has been developed by Prof. P. Chatterjee to analyze the transport properties of a device as a function of position [1]. Initially, it was conceived to model amorphous device and

it was extended later to crystalline silicon cells and HIT structures [12]. This program includes the electrical and optical parts.

The electrical part is based on the Poisson's equation and hole and electron continuity equations. These three equations are solved simultaneously under non equilibrium steady state condition.

At thermodynamic equilibrium, only the Poisson's equation has to be solved

$$\frac{\partial^2 \psi(x)}{\partial x^2} = -\frac{\rho(x)}{\varepsilon}, \quad (7)$$

where ε is the dielectric constant, $\rho(x)$ is the net charge density and $\psi(x)$ is the value of the vacuum level at some point x of the device. The dependent variable is $\psi(x)$, and it is calculated using the finite difference and the Newton-Raphson method. The initial guess for $\psi(x)$ is a straight line appending the boundary values.

This initial guess for $\psi(x)$ is used to calculate the initial value of the Fermi level position measured from the valence band given by

$$E_F - E_v = -\chi(L) - \Phi_{bL} - \psi(x) + \chi(x) + E_g(x). \quad (8)$$

Here, $\chi(L)$ is the electron affinity at $x = L$, where L is the length of the device, Φ_{bL} is the distance in energy from the Fermi level to the conduction band, $\chi(x)$ and $E_g(x)$ are, respectively, the electron affinity and gap energy at some point x . Here, $\psi(x) = 0$ is chosen to be the position in energy of the vacuum level at $x = L$.

This value of the Fermi level enables to calculate the occupation functions of the amphoteric dangling bonds in each charge state, the defect density $D(E)$, its three components D^+ , D^0 , D^- and trapped electrons and holes. Then, a better estimate of $\psi(x)$ is calculated and used for another iteration. The procedure is continued until the convergence, the criterion of which is taken to be equal to 10^{-9} at thermodynamic equilibrium. The DPM has not been inserted in ASDMP at non-thermodynamic equilibrium yet.

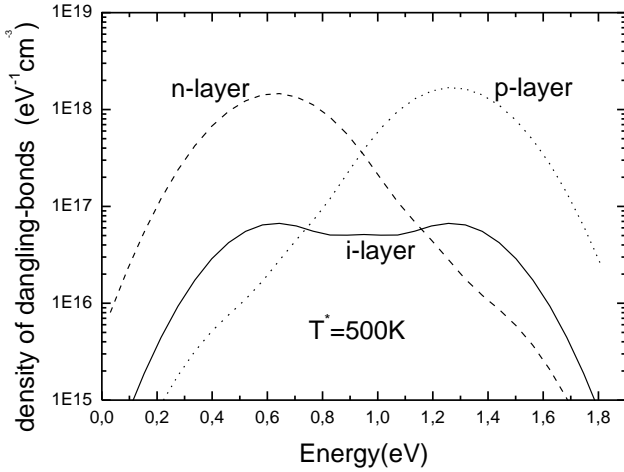
4. RESULTS AND DISCUSSION

In this section, we describe and discuss the results obtained by ASDMP for a solar cell based on a standard p-i-n structure. Using both the defect pool model (DPM) and the standard model (SM), we analyze the distribution of the defects in mobility gap and its effects on the output parameters at thermodynamic equilibrium. For our calculation, we have adopted a set of standard parameters typical for good quality a-Si:H. They are summarized in Table 1.

Fig. 1 shows the defect state density versus the energy for three positions in the device located in p-layer, i-layer and n-layer. The position of the Fermi level affects the defect distribution. The DB in n-layer are condensed in the lower region of the gap, while those of the p-layer are in the upper part. Additionally, we can see that the values of DOS in the doped layers $\sim 10^{18} \text{ eV}^{-1} \text{ cm}^{-3}$ are much higher than in the intrinsic one $\sim 5.10^{16} \text{ eV}^{-1} \text{ cm}^{-3}$.

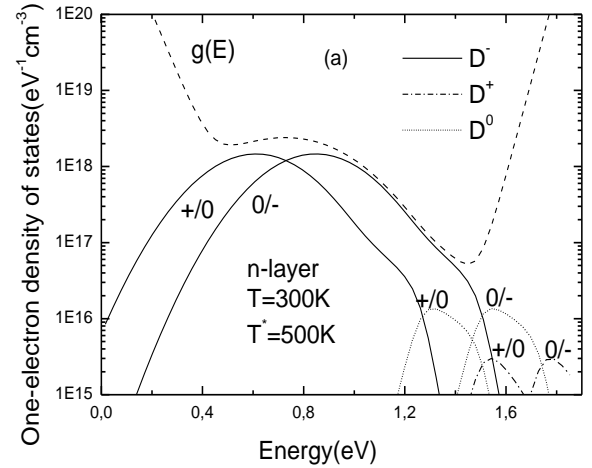
Table 1 – Standard parameters used for calculation of defect distribution

Parameters	Standard Model(SM)			Defect Pool Model(DPM)		
	P	i	n	p	i	N
Layer						
Mobility gap (E_g)(eV)	1.9	1.9	1.9	1.9	1.9	1.9
Layer Thickness X (nm)	14	700	14	14	700	14
Electron affinity χ (eV)	3.89	3.9	4.0	3.89	3.9	4.0
Characteristic energy VB tail E_{V0} (eV)	0.055	0.045	0.055	0.055	0.045	0.055
Characteristic energy CB tail (eV)	0.035	0.025	0.035	0.035	0.025	0.035
Switched energy (eV)	0.89	0.89	0.89	---	---	---
Effective DOS in valence and conduction bands (cm^{-3})	2.10^{20}	2.10^{20}	2.10^{20}	2.10^{20}	2.10^{20}	2.10^{20}
Exponential tail Prefactors N_{V0}, N_{c0} (cm^{-3})	4.10^{21}	4.10^{21}	4.10^{21}	4.10^{21}	4.10^{21}	4.10^{21}
Donor/Acceptor doping (cm^{-3})	1.10^{18}	--	1.10^{18}	1.10^{18}	---	1.10^{18}
Equilibrium Fermi level (eV)	0.80	1.05	1.30	---	---	---
Energy Separation Δ (eV)	---	---	---	0.44	0.44	0.44
Pool peak position E_p (eV)	---	---	---	1.27	1.27	1.27
Pool width σ (eV)	---	---	---	1.85	1.78	1.85
Hydrogen concentration H (cm^{-3})	---	---	---	5.10^{21}	5.10^{21}	5.10^{21}
Correlation energy U (eV)	0.5	0.5	0.5	0.2	0.2	0.2
Defect state density freeze-in temperature T^* (K)	---	---	---	500	500	500
Total DOS under the donor/acceptor Gaussian (cm^{-3})	8.10^{18}	8.10^{18}	8.10^{18}	---	---	---
Position of donor Gaussian peak from E_v (eV)	0.75	0.75	0.75	---	---	---
Position of acceptor Gaussian peak from E_c (eV)	0.65	0.65	0.65	---	---	---
N^0 of Si-H bonds involved by every reaction i	---	---	---	2	2	2

**Fig. 1** – Calculated density of dangling bond states in three positions of a p - i - n solar cell. These DOS are maintained at temperatures above the equilibrium temperature T^*

The one-electron density of states is given by the expression $g(E) = D(E + kT \ln(2)) + D(E - U - kT \ln(2))$, where $g(E)$ depends on T even when $D(E)$ does not. In Fig. 2 we present $g(E)$ and its components for the same positions as above in n and p layers at $T = 300$ K. Fig. 2 shows that in n -layer (a), the positions of neutral and positively charged defects are shifted to higher energies, while in p -layer (b), they are positions of neutral and negatively charged defects which are shifted to lower energies. These results obtained by ASDMP for a p - i - n structure are similar to the ones obtained by Powell and Deane for doped and undoped materials.

The value of the energy separation between the doubly occupied D^- state in n -type and the empty D^+ state in p -layer Δ is well-known experimentally. We have taken $\Delta = 0.44$ eV [13]. For the correlation energy,

**Fig. 2** – One-electron density of states and their components formed at equilibrium temperatures as D^+ , D_0 , D^- calculated in two positions of the p - i - n solar cell

we have taken the commonly used value of 0.2 eV. But the value of the pool width σ is less known, so the program calculates the value of σ , which gives an energy separation of $\Delta = 0.44$ eV.

The electric fields calculated using both the SM and DPM are compared in Fig. 3. We can see that the DPM leads to a stronger field near the p/i and i/n interfaces. This field is lower in the bulk. In this case, there is an excess of hole trapping near the p/i interface leading to a high positive charge and electron trapping near the i/n one leading to a high negative charge. Consequently, strong electric fields are developed near the interfaces and, obviously, the bulk field becomes lower. For these reasons, the band diagrams plotted in Fig. 4 are flatter in the bulk when they are calculated from the DPM.

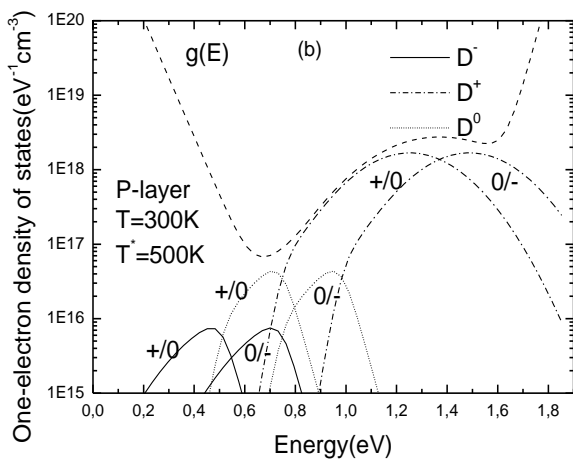
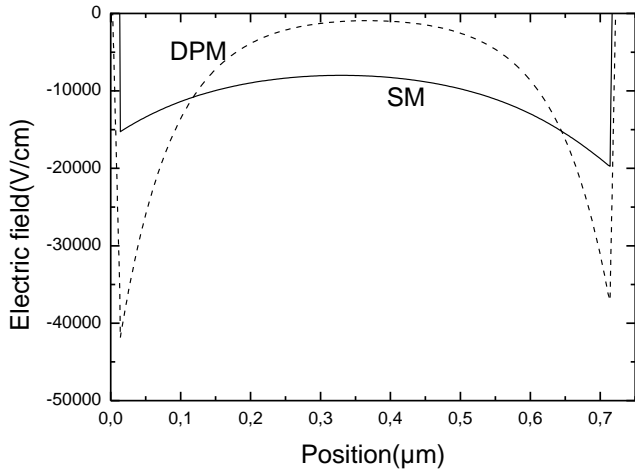


Fig. 3 – The electric field within the device calculated with both the SM and DPM at the thermodynamic equilibrium. $T = 300$ K, $T^* = 500$ K

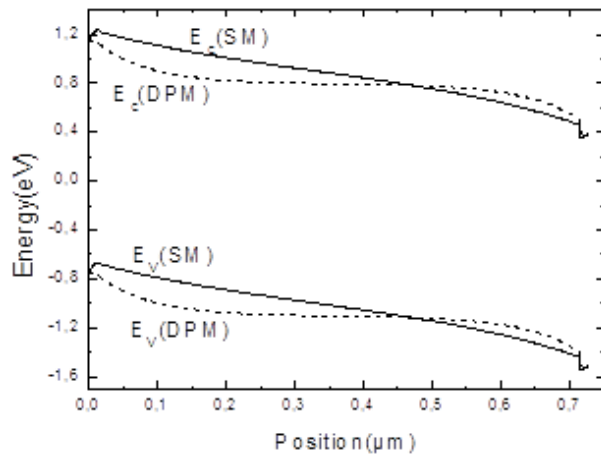


Fig. 4 – Band diagrams calculated from both the SM and DPM under thermodynamic equilibrium $T = 300$ K, $T^* = 500$ K

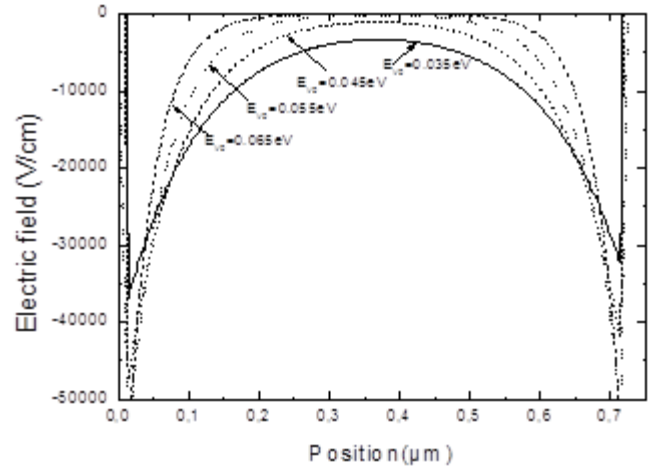


Fig. 5 – The electric field within the device calculated with different values of characteristic energy E_{v0}

Now, we consider the effect of the slope of the valence band on the electric field. In Fig. 5 we have plotted the electric field versus the position in the structure for different values of the slope of the valence band E_{v0} . When E_{v0} rises, the electric field increases near the interfaces and decreases in the bulk. This is obvious since the augmentation of E_{v0} leads to a greater density of defects (Eq. (3)) and then to an increase in carrier trapping.

5. CONCLUSIONS

Using the concept of the defect pool, we have formed a numerical model and inserted it in ASDMP at thermodynamic equilibrium. We have calculated the density of states in each position of a standard solar cell based on *p-i-n* structure. The doping causes an increase in the dangling bond density and the distribution of these DB is affected by the Fermi level position. We have calculated the one-electron density of states both in *n*-type and *p*-type layer. In *n*-type, neutral and positively charged defects are shifted to higher energies and in *p*-type, neutral and negatively charged defects are shifted to lower energies. We showed that negatively charged defect transitions in *n*-type material occur at lower energy than positively charged defect ones in *p*-type material.

We have compared the output parameters obtained from the SM and DPM. Using the DPM, we found that in the intrinsic layer, near the interfaces, electric field is stronger and the band diagrams are more bonded. In the bulk, the field decreases and the bands become flatter. This has been explained by the high density of trapped charges near the interfaces. This behavior of the electric fields is accentuated when the slope of the valence band increases. This is because the defect density becomes higher leading to an excess of carrier trapping.

REFERENCES

1. M. Nath, P. Chatterjee, J. Damon-Lacoste, P. Roca i Cabarrocas, *J. Appl. Phys.* **103**, 034506 (2008).
2. U. Dutta, P. Chatterjee, S. Tchakarov, *J. Appl. Phys.* **98**, 044511 (2005).
3. R. Biswas, B.C. Pan, *J. Non-Cryst. Solid.* **299-302**, 507 (2002).
4. K. Morigaki, H. Hikita, *J. Non-Cryst. Solid.* **266-269**, 410 (2000).
5. N. Powell, R.B. Wehrspohn, S.C. Deane, *J. Non-Cryst. Solid.* **299-302**, 556 (2002).
6. H.M. Branz, *J. Non-Cryst. Solid.* **266-269**, 391 (2000).
7. A.F. Bouhdjar, L. Ayat, A.M. Meftah, N. Sengouga, A.F. Meftah, *J. Semicond.* **36**, 014002 (2015).
8. A.F. Meftah, A.M. Meftah, A. Merazga, *Defect Diffusion Forum* **230-232**, 221 (2004).
9. D. Reaux, J. Alvarez, M.E. Gueunier-Farret, J.P. Kleider, *Energy Procedia* **77**, 153 (2015).
10. M.J. Powell, S.C. Deane, *Phys. Rev. B* **53**, 10121 (1996).
11. M.J. Powell, S.C. Deane, *Phys. Rev B* **66**, 155212 (2002).
12. M. Rahmouni, A. Datta, P. Chatterjee, J. Damon-Lacoste, C. Ballif, P. Roca i Cabarrocas, *J. Appl. Phys.* **107**, 054521 (2010).
13. K. Pierz, W. Fuhs, H. Mell, *Philos. Mag. B* **63**, 123 (2006).

Defect Pool Numerical Model in Amorphous Semiconductor Device Modeling Program

M. Rahmouni, S. Belarbi

Université des Sciences de la Technologie Mohamed-Boudiaf, El Mnouar, BP 1505, Oran, Algeria

Програма моделювання аморфних напівпровідникових приладів (ASDMP), розроблена професором P. Chatterjee і широко підтверджена експериментальними результатами, є детальною програмою, де рівняння Пуассона і рівняння безперервності електронів і дірок розв'язуються одночасно без жодного спрощення. Вона враховує кінетику захоплення і рекомбінації через стани у забороненій зоні. У цій програмі щільність станів моделюється за допомогою стандартної моделі (SM). Така модель описує дефекти двома гаусіанами поблизу центра забороненої зони та двома хвостами, експоненціально розподіленими за енергією, і припускає, що щільність станів однорідна у просторі. Defect pool model (DPM) є вдосконаленою моделлю формування дефектів у гідрогенізованому аморфному кремнії на основі ідеї, що сітка неупорядкованих атомів a-Si:H має великий спектр локальних середовищ, в яких може бути сформований дефект. Таким чином, ці дефекти вибирають місця, де їх енергія утворення мінімальна, і це стає можливим з рухом водню.

Використовуючи підхід до опису дефектів, ми розробили чисельну DPM і застосували її у ASDMP при термодинамічній рівновазі. Ми використали ASDMP, щоб отримати щільність станів у кожній позиції сонячного елемента на основі стандартної структури *p-i-n*. Показано вплив допінгу на концентрацію дефектів та досліджено вплив положення рівня Фермі на розподіл щільності станів. Ми визнали використання ASDMP ключовим результатом того, що негативно заряджені дефекти в матеріалі *n*-типу розташовані нижче за енергією, ніж позитивно заряджені дефекти в матеріалі *p*-типу, навіть якщо енергія кореляції позитивна.

Ми розраховували електричне поле і діаграми смуг при термодинамічній рівновазі як з DPM, так і з SM. Ми показали, що електричне поле, отримане від DPM, сильніше поблизу інтерфейсів і нижче в об'ємі, де діаграми смуг більш плоскі. Така поведінка електричного поля, розрахованого за даною моделлю, підкреслюється зі збільшенням нахилу хвостів валентної зони.

Ключові слова: Hydrogenated amorphous silicon, Defect pool model, *p-i-n*.